Slow dynamics of photospheric regions of the open magnetic field of the Sun, solar activity phenomena, substructure of the interplanetary medium and near-Earth disturbances in the beginning of the 23rd cycle: 1. The December 1996–February 1997 events

K. G. Ivanov,[1] V. Bothmer,[2] P. J. Cargill,[3] A. F. Kharshiladze,[1]

E. P. Romashets,[1] and I. S. Veselovsky [4]

Short title: SLOW DYNAMICS OF PHOTOSPHERIC REGIONS

[1] Institute of Terrestrial Magnetism, Ionosphere, and Radio Wave Propagation, Troitsk, Moscow Region, Russia
[2] Max-Plank Institut für Aeronomie, Katlenburg-Lindau, Germany
[3] Imperial College of Science, Technology, and Medicine, London, UK
[4] Moscow State University, Russia

Abstract. Slow (from one rotation to another) dynamics of photospheric regions in the open lines of the solar magnetic field (OR), its relation to the dynamics of photospheric coronal manifestations of solar activity and to the substructure of the coronal magnetic field and interplanetary medium are considered in the minimum of the 23rd cycle of solar activity. It is shown that the OR convergence was accompanied by a generation (decay) of the unstable large-scale configuration of the coronal field on the source surface and of the complex of solar activity phenomena related to the latter. Occurrence (attenuation) of the intense solar-interplanetary disturbance on 5–15 January 1997, was a manifestation of this instability. Solar and near-Earth observations of this disturbance are analyzed, taking into account previous studies to develop more detailed scenario of its development, formulate stronger restrictions on setting the conditions for MHD-modeling and to test its results. It is shown that there exists a configuration problem in understanding of a near-Earth disturbance. An application of models of a super-expanding cloud in a two-velocity solar wind [*Schmidt and Cargill*, 2001] may be one of the ways to solve the problem. In the scope of the scenario suggested, such specific features of this disturbance as the unusually large jump of the plasma density at the cloud rear wall [*Fox et al.,* 1998], kilometer radio burst of type II with a fast frequency drift [*Reiner et al.,* 1998], anomalous Forbush-effect during the cloud passage and strong north-south anisotropy of cosmic rays at the disturbance development phase (a heliospheric substorm) find their qualitative explanation [*Bieber and Evenson,* 1998].

1. Introduction

Currently a considerable attention is paid to the study of complex streams of the interplanetary plasma from complex sources [*Bravo et al.,* 1998; *Burlaga et al.,* 1987; *Crooker and McAlister,* 1997; *Dryer,* 1974; *Dryer and Smith*, 1987; *Gonzalez et al.,* 1996; *Gosling*, 1993; *Ivanov,* 1996, 1998; *Mogilevsky et al.,* 1997]. These complex solar sources are presented, as a rule, as all possible combinations of flare-active regions, filaments, coronal holes, and streamers and in the solar physics are often called solar activity complexes [*Mogilevsky et al.,* 1997]. It has been assumed for a long time that the large-scale hydrodynamic circulation is responsible for solar activity complexes in the convective zone of the Sun [*Bumba,* 1987; *Bumba and Howard*, 1965; *Starr and Fisher,* 1971; *Ward,* 1964, 1965]. The indications have been obtained recently that the dynamics of photospheric regions of the open magnetic field of the Sun is a convenient indicator of this hydrodynamic circulation at temporal scales from one to several solar rotations [*Ivanov and Kharshiladze*, 2002; *Ivanov et al.*, 2001b]. In particular, this dynamics points to interactions between large-scale hydrodynamic streams (possibly, between the giant modes of the convective instability), the solar activity complexes arising and disappearing in the acts of mutual collision and reflection of these streams, respectively.

Thus the use of slow (from one rotation to another) dynamics in an ensemble of photospheric regions of the open field of the Sun, interpretation of this dynamics as an indicator of hydrodynamic interactions, and discovery of its close relation to generation and decay of solar activity complexes make it possible to analyze the solar-terrestrial relations in a wider chain of interrelated phenomena: hydrodynamic processes in the convective zone → dynamics of the photospheric regions of the open field of the Sun → solar activity complexes (complicated solar sources) → complex streams of the interplanetary magnetoplasma. One can made this analysis more systematic presenting the subsector structure of the coronal and interplanetary magnetic field as a corresponding continuation of en-

sembles of photospheric regions of the open field of the Sun [*Ivanov et al.,* 2001a; *Levine et al.,* 1977]. Some prominent solar-terrestrial phenomena in 1997 and 1999–2000 have been already considered from this point of view [*Ivanov and Kharshiladze*, 2002; *Ivanov et al.,* 2001a, 2001b]. The relations of the dynamics of the photospheric region of the open field of the Sun to solar activity phenomena, substructure of the coronal magnetic field and interplanetary medium during three solar rotations in December 1996–February 1997 are studied in this paper. Some sort of an apotheosis of these phenomena was a prominent event in the solar-terrestrial physics on 6–11 January 1997, many interesting papers being dedicated to this event entirely or partially [*Berdichevsky et al.,* 2000; *Bieber and Evenson*, 1998; *Bruckner et al.,* 1998; *Burlaga et al.,* 1998; *Canfield et al.,* 1999; *Cid et al.,* 2001; *Farrugia et al.,* 1998; *Fox et al.,* 1998; *Funsten et al.,* 1999; *Hidalgo et al.,* 2000; *Hudson et al.,* 1998; *Ivanov*, 2000; *Ivanov and Romashets*, 1997, 2001; *Ivanov et al.,* 2001a; *Kaiser et al.,* 1998; *Lewis and Simnett,* 2000; *Reiner et al.,* 1998; *Sheeley et al.,* 1999; *Shodhan et al.,* 2000; *Subranian et al.,* 1999; *Tsurutani et al.,* 1998; *Watari and Watanabe,* 1998; *Webb et al.,* 1998; *Wu et al.,* 1999; *Zhao and Hoeksema*, 1997].

2. Data and Methods

The measurements of the photospheric magnetic field at the Wilcox Solar Observatory [http://quake.Stanford.edu/∼wso] were used to determine spherical coefficients of the Gauss series in one of the versions of the solar magnetic field potential model with a surface source [*Kharshiladze and Ivanov*, 1994] and to further project the open lines from the source surface onto the photosphere by the *Levine et al.* [1977] method. That is the way the maps of photospheric regions of the solar magnetic field were obtained (Figure 1). Then the photosphere surface in the Mercator projection was split to rectangles by the system of parallels and meridians drawn per 18 and 36 degrees, respectively. Rectangles

ik were numbered from East to West ($i = 0, 1, ..., 9$) and from North to South ($k = 0, 1, ..., 9$). Using this rectangle grid, a computer was memorizing the position of the photospheric ends of open lines. This made it possible, projecting photospheric regions onto the source surface, to obtain a subsector structure of the coronal magnetic field with known positions of the photospheric "sources" of corresponding subsectors (Figure 2). The following information was also plotted onto the above-described maps: (1) the boundaries of coronal holes according to the observations in the Fe XIV line at the Sacramento Peak observatory, the magnetic field of spot groups according to the observations at the Kitt Peak observatory, and also the active filaments (Solar-Geophysical Data, 1997) (Figures 3–4).

Later on, for the sake of convenience the open lines of the solar magnetic field (OR) outgoing from various photospheric latitudes will be called polar (k = 0–1; 8–9; $|\Phi| = 54 - 90°$), midlatitude ($k = 2; 7$; $|\Phi| = 36 - 54°$), low-latitude ($k = 3; 6$; $|\Phi| = 18 - 36°$), and near-equatorial ($k = 4; 5$; $|\Phi| = 0 - 18°$). Here Φ is the heliogeographic latitude; k is the index in the ik rectangles which the photosphere was split to. The measurements of the magnetic field and plasma on board the Wind space vehicle (leading experimenters were R. Lepping and K. Ogilvie, http://cdaweb.gsfc.nasa.gov) were used to identify and analyze the subsector structure of the interplanetary plasma and complex streams of the interplanetary magnetoplasma.

3. Photospheric Regions of the Open Lines of the Solar Magnetic Field

Figure 1 shows the photospheric regions of the open lines of the solar magnetic field (small circles) for three consequent rotations of the Sun centered at 13 December 1996, 9 January 1997, and 5 February 1997. One can arrive to the following qualitative conclusions

on the structure, configuration, and dynamics of the open region (we will designate them as OR).

The 13 December Rotation. (1) There are two vast high-latitude and three low-latitude OR. (2) The longitudinal distribution of the stream in the high-latitude OR is inhomogeneous: there are pairs of "tongues" of open lines in each polar cap, the tongues being aligned toward middle latitudes in the Northern hemisphere and remaining in the polar zone in the Southern hemisphere.

Table 1 shows the shortest distances r between the centers of the low-latitude OR and the ends of the high-latitude "tongues." All the distances between OR and "tongues" of opposite and same polarity are larger and less than the radius of the Sun, respectively (according to the terminology proposed by *Ivanov et al.* [2001b], these distances characterize remote and close interactions between OR). During the rotation of the Sun from 13 December to 9 January, the $+1/+2$ and $-3/-4$ OR pairs united and are designated below as $+1^*$ and -3^*, respectively (Table 1, Figure 1).

The 9 January Rotation. We draw attention to the fact that a considerable decrease of the mutual distance in the $+3/-2$ and $+3/-3^*$ pairs occurred in this rotation (Figure 1, Table 1). This means that there occurred a convergence of the photospheric bases of the open field lines (interaction of collisions according to *Ivanov et al.* [2001b]). This fact is important for the following interpretation of the causes of the 6–11 January 1997 disturbance generation from both the phenomenological (it is shown below that this convergence was accompanied by a specific dynamics of the coronal field subsector structure and appearance of a complex of activity phenomena) and physical (the convergence of the photospheric bases of open field lines may lead in principle to a destabilization of the large-scale configuration of the coronal field [*Forbes and Priest,* 1995]) points of view.

The 5 February rotation. In this rotation the distance in the $+3/-2$ and $+3/-3^*$ pairs increased significantly as compared to the previous rotation (Table 1); an OR reflection from each other occurred and this, as it is shown below, was accompanies by a weakening of the photospheric and coronal activity in the space between these OR.

4. Photospheric Open Regions and the Subsector Structure of the Coronal Magnetic Field

Figure 2 shows the subsector structure of the coronal magnetic field with the sector and intersector boundaries in a sequence of three solar rotations. One can see that this structure is complex and dynamical:

1. The coronal and therefore interplanetary field on the source surface, in particular near the equator at the Earth's helioprojection, appears to be formed by both the low-latitude photospheric regions and magnetic field lines outgoing from the high-latitude photosphere (from the polar caps). The photosphere high-latitude field penetrates to the equator at coronal heights and is here adjacent to the field coming from the near-equatorial photosphere. *Levine et al.* [1977] was the first to pay attenuation to this fact and to use it to interpret some observed high-velocity streams of the solar wind at the Earth's orbit. We suggest [*Ivanov et al.,* 2001a] to consider also the intersector boundaries as absolutely real physical and (possibly) geoeffective objects, since these boundaries and the sector boundary are based on the same theoretical model, and objectivity and geophysical significance of sector boundaries arise no doubts since long ago.

2. In the section of the solar disk considered, the Earth's helioprojection crosses in sequence 5–6 subsectors limited by two parts of the sector boundaries (HCS) and by two–three intersector boundaries (SB) (Table 2). Below we pay a special attention to the SB boundary observed in sequence on 10 December, 7 January, and 3 February since: (a) it

was the most nonequilibrium in the sense that it separated open fields coming from the near-equatorial and high-latitude photosphere; (b) near it the subsector structure was the most dynamic, that is the structure included a small subsector of open lines of the southern polar zone (−2), the distance to which had a positive correlation with the convergence–divergence in the $+3/-2$ photospheric OR pair (Table 1); (c) at this boundary and near it, there occurred a complex of solar activity phenomena (active regions, active filaments, and a nonstationary coronal hole) which caused the 6–11 January 1997 disturbance; (d) at least, as *Ivanov et al.* [2001a] suggested, this very boundary behaved in the near-Earth disturbance as a stream interface with an exceptionally large increase of the solar wind proton concentration and a pulse of the dynamical pressure onto the magnetosphere.

We explain in detail point (b). It was noted in Section 3 that a mutual convergence and divergence was observed in the sequence of three rotations in the $+3/-2$ photospheric OR pair (Table 1). This convergence is interpreted preliminarily as an indicator of the large-scale MHD-interactions [*Ivanov et al.,* 2001b]. The fact that the corresponding subsectors of the coronal magnetic field are located close to each other (Figure 2), though the photospheric OR are significantly separated from each other (Figure 1), confirms the assumption on the interaction. Moreover the mutual distance between the subsectors varies in parallel with the convergence–divergence of the corresponding photospheric OR. At the phase of the strongest convergence (the 9 January rotation) the subsectors touch each other and there arises a "joint" between the corresponding intersector boundaries and HCS. *Ivanov and Kharshiladze* [2002] drew attention to similar "joints" (in particular during the prominent events on July 2000), as to a formation of a potentially unstable geo-effective large-scale configuration of the solar magnetoplasma, a destabilization of which is accompanied by powerful sporadic phenomena. In the cause in question (see below) AO SN84 with a series of suddenly disappearing filaments that led to the 6–11 January 1997 events [*Webb et al.,* 1998] were observed just at a "joint." Simultaneously with the

convergence–divergence in the OR $+3/-2$ pair, there occurred a collision–reflection in the $+3/-3^*$ pair (Figure 1, Table 1), and this resulted in a strong shift of OR +3 southward with the strongest in these three rotations HCS deformation. Possibly it was one of the causes of the large-scale field destabilization. A signature of the latter was the formation of a small nonstationary low-latitude coronal hole that contributed significantly to the January disturbance [*Burlaga et al.,* 1998]. Moreover a photospheric OR convergence occurred in the $+1^*/-2$ (9 January rotation) and $1^*/+3$ (5 February rotation) pairs (Table 1). The convergence was accompanied by rearrangements of the coronal field subsector structure and an increase of the solar activity in the space between OR (for example, AO NOOA 8009 occurrence during the convergence in the $+1^*/-2$ pair). These problems are considered in more details in the following section.

5. Open Photospheric Regions and Solar Activity Phenomena

Figure 3 shows the distribution of photospheric OR and solar activity phenomena (CH coronal holes according to observations in the Fe XIV green line, active regions, and filaments). No optical flares of $I \geq 1$ class were observed in this period. It is worth noting also that *Watari and Watanabe* [1998] presented the data on coronal holes based on the observations in the soft roentgen at the SXT/Yokou spacecraft which show a slightly different picture than that in Figure 3: the roentgen CH covered not only high latitudes but also almost the entire low-latitude subsector +3 (Figure 2).

Now we consider the dynamics of solar activity phenomena in the space (the interaction region according to *Ivanov et al.* [2001b]) between OR $+3/-2$, $+3/-3^*$, and $+1^*/-2$.

The OR $+3/-2$ pair was marked in previous paragraph as related to the solar-interplanetary disturbances on 6–11 January 1997. Figure 3 confirms that at a convergence

of open regions of this pair (the 9 January rotation), AO NS84 reached its maximum development evaluated by bipolar group fields and filament activity [*Webb et al.,* 1998], these phenomena becoming one of the main causes of the January disturbances. In this period AO SN84 is located most close to OR +3 occupied by a roentgen coronal hole [*Watari and Watanabe,* 1998]. The interaction between AO and CH could [*Vorpahl and Broussard*, 1978] lead to a filament ejection [*Webb et al.,* 1998] and nonstationary of CH in the southern part of the roentgen CH [*Watari and Watanabe*, 1998], i.e. to the appearance at this place of a transient CH in the helium line [*Burlaga et al.,* 1998]. After mutual divergence in the OR $+3/-2$ pair, the situation relaxed to a more quiet level (Figure 3, the 5 February rotation): the helium hole disappeared, the active region almost decayed, and filament ejections stopped. During the entire rotation, there exists in the interaction region of the $+3/-3^*$ pair an active filament perpendicular to HCS (Figure 3). AO NOOA 8009 arises in the interaction region of OR $+1^*/-2$ during their convergence (Figure 3, the 9 January rotation). Thus the assumption that in an ensemble of photospheric OR there exist pair interactions manifested in generation (attenuating) of solar activity phenomena during their mutual convergence (divergence) is confirmed.

Figure 4 confirms this assumption demonstrating that solar activity phenomena have a tendency to appear not only near sector boundaries (this has been known for a long time) but near intersector boundaries as well.

Actually, the following facts should be noted: 1) Low-latitude holes in the 13 December rotation appear near HCS$(-0/+1)$ and SB$(+1/+0)$, whereas AOSN 84 appears near SB$(-1/-0)$. 2) During the 9 January rotation, AO SN84 occurs at the "joint" of HCS and two intersector boundaries whereas low-latitude CH (one of them — in the He 10830 line) occur at intersector boundaries SB$(+1^*/+1^*a)$ and SB$(1^*/+3)$. 3) During the 5 February rotation, AO 8014 arises at the joint of HCS$(-0/+1^*)$ and the SB$(-0/-1)$ intersector boundary, and the tongue of the polar CH and AO NOOA 8009 is located at

the SB($1^*/+1^*a$) boundary.

6. The Subsector Structure of the Interplanetary Medium

Figures 5–10 show the variations of the 1-minute average values of the interplanetary magnetic field (IMF) components B, B_x, B_y, and B_z, stream velocity components V_x, V_y, and V_z, thermal velocity V_T, and concentration n of the solar wind protons according to the measurements in the near-Earth interplanetary medium on board the Wind satellite. These variations characterize the magnetoplasma streams coming to the Earth from the part of the solar disk considered above (Figures 1–4) in a sequence of three solar rotations. These variations make it possible to consider three different states of the interplanetary medium within four boundaries. We assume that these states and boundaries are interplanetary manifestations of the coronal field subsector structure (Figures 2, and 4), i.e. of three subsectors out from the ones considered above and of four boundaries (two sector and two intersector ones).

Subsectors in IMF are determined on the basis of a high level of fluctuations (especially in the field components) within subsectors and an attenuation of these fluctuations between subsectors. As for the boundaries, sector ones are determined confidently enough by the change of the IMF B_x and B_y signs, whereas an accurate determination of intersector boundaries still remains problematic. Evidently, there is a multiformity of intersector boundary types. It was noted earlier [*Ivanov et al.,* 2001b] that SB1 and SB2 intersector boundaries in the 9 January rotation (Figures 6, and 9) present a stream interface [*Burlaga et al.,* 1998] and a wide transition between the third and following subsectors, respectively.

Subsectors in variations of the solar wind parameters were determined first in the same way as in the IMF by high and low intensity of fluctuations of the stream velocity

components V_x, V_y, and V_z within and between subsectors, respectively, and second by similar variations of the proton temperature and its fluctuations (Figures 8–10). In all rotations the SB1 intersector boundary coincided to or existed near the stream interface, whereas the SB2 boundary presented a wide transition.

The interplanetary disturbances in the beginning of January 1997 are below studied in detail.

7. The Interplanetary Disturbances on 7–14 January 1997

As it has been mentioned above, many authors had studied these disturbances from various points of view. We presented above the arguments in favor of the concept that the slow global processes in convective zone which are manifested in the dynamics of the photospheric regions of the open magnetic field of the Sun were able to prepare in advance the complex of the solar activity phenomena which became an indirect cause of these disturbances. We would like to demonstrate that in principle the chain of solar-terrestrial phenomena usually attracted to analyze a complex of interplanetary disturbance in a particular period of time may be extended in the direction of more fundamental, global, and taken in advance solar activity phenomena.

On the other hand, paying a respect to many particular results the studies of these disturbances, we would like to pay attention to some additional possibilities of specification and concretization of our views on the dynamics, structure, and configuration of both the solar source of these disturbances and their near-Earth manifestations. This would make it possible to set initial conditions for the MHD-modeling based on the data on this source and to carry out a testing of models based on the data on the near-Earth disturbance.

We begin to discuss the conditions which the modeling of a near-Earth disturbance should satisfy to. Ultimately the theoretical model should provide an agreement to: (1) the

data on the configuration (in particular to the observed directions of the normals to main boundaries); (2) the IMF profiles obtained by sounding of the magnetic cloud by near-Earth space vehicles; (3) the real position of the forward shock wave relative the cloud magnetopause; (4) the observed unusually large pressure pulse (proton concentration) on the stream interface of the disturbance; (5) the anomaly Forbush-effect in galactic cosmic rays registered during the cloud passage; and (6) the data on kilometer radioemission of the II type. Even when these data are satisfied to, the model has to reproduce accurately the velocity field around and within the cloud and also take into account the average (cleared from fluctuations) external IMF, its transition across the forward front, the draping near the cloud, the nonlinear character of the IMF fluctuations, their transformation at the shock wave front and interaction with the cloud.

7.1. Disturbance Configuration: The Direction of Normals

Table 3 shows determinations of the solar-ecliptic angles of normals $\varphi_{\rm N}$, $\theta_{\rm N}$ to the main boundaries of the near-Earth interplanetary disturbance on 9–11 January 1997: to the shock wave front S_f; to a pair of strong discontinuities (possibly tangential) within the shock layer TD_1 and TD_2; to the strong discontinuities in the vicinity of the cloud magnetopause TD_3, TD_4, and R_1; to the front and rear walls of the density pulse on the stream interface SI_1 and SI_2; to the structural element called a "magnetic hole" MH by *Burlaga et al.* [1998]; and to the front rotational discontinuity RD_f [*Ivanov and Romashets*, 1997].

The normal to S_f was determined by three methods: the kinematics [*Safrankova et al.,* 1998], "optimal" [*Berdichevsky et al.,* 2000], and standard method of transition matrix. The latter method was used also to determine normals to TD_1, TD_2, TD_3, R_1. MH, and RD_f. The kinematics method was applied to estimate normals to SI_1 and SI_2.

Table 3 shows that normals to all the boundaries in the front part of the disturbance (from the shock wave front S_f to the stream interface SI, MH) are almost parallel to each other. The average direction is $\varphi_N = 210°$, $\theta_N = -25°$, the normal to RD_f not being taken into account.

Thus one of the requirements to a real modeling of this disturbance is that its local configuration near the Earth should satisfy this average direction of the normal. Hence it follows also that the main structural regions of the MHD-disturbance (the shock wave, cloud, stream interface) were extended between the second and fourth quadrants on the $Z = 0$ plane of the solar-ecliptic coordinate system, and on the whole the disturbance propagated from the north-east to the south-west.

7.2. The Disturbance Configuration and the IMF Profiles in the Magnetic Cloud

It is known that in principle configuration characteristics of a magnetic cloud may be found in the class of acceptable geometric bodies by solving the inverse problem, based on the experimental data on profiles of the magnetic field components obtained in cloud sounding by space vehicles. However this problem is ambiguous because of the necessity to vary both, the body form and sounding trajectory, as well as the distribution of electric currents. Therefore solving such problems, one has to be careful and to take into account maximally independent data on the disturbance configuration. The data may be obtained in particular from the experimental determination of normals to the main boundaries of the front part of the disturbance (Table 3).

Table 4 shows the results of two known solutions of inverse problems in the class of round cylinders with radius R_0, the trajectory line-of-aim Y_0, and the cylinder (clouds) axes in the directions φ_a, θ_a, applied to the IMF component profiles obtained on board the

Wind satellite on 10–11 January 1997. A powerless configuration of the current [*Burlaga et al.*, 1998] was taken in one case. In the other case the toroidal and poloidal components of the current were distributed homogeneously along the sounding trajectory [*Hidalgo et al.,* 2000]. In the latter paper, the corresponding values of the normals φ_N and θ_N to the boundary in the point of the trajectory entry into the cloud unambiguously determined from the values of φ_a, θ_a, R_0 and Y_0 are also presented.

One can see from Table 4 that the line-of-aim distances differ by a factor of five in spite of the fact that in both solutions the parameters φ_a and θ_a are very close to each other. However it is significant that these solutions lead to values $\varphi_N = 165^\circ$ and $\theta_N = 20^\circ$ which do not agree with the strongest experimental limitations on possible models, that is with the real configuration of the frontal part of the disturbance in which normals to all main boundaries are oriented on average along the direction $\varphi_N = 210^\circ$ and $\theta_N = -25^\circ$ (Table 3). We think that this contradiction is due to the fact that in principle, solving inverse problems, one should take into account, first, the magnetic field of the electric currents at the cloud boundary and, second, possible cloud deformations with a strong deviation of its form a cylindrical one [*Cargill et al.,* 2000; *Odstrcil and Pizzo*, 1999; *Riley et al.,* 1997; *Schmidt and Cargill,* 2001; *Wu et al.,* 1999].

In relation to this, the model of evolution of a super-expanding magnetic cloud in a two-velocity solar wind [*Schmidt and Gargill,* 2001] may be of a special interest for explanation of the above-discovered discrepancy. In this model: one part of the cloud is located in the slow stream of the solar wind and the other part is in the fast stream; there is mainly a meridional expansion of the cloud with a formation of a narrow neck at the boundary between the fast and slow streams, and with a strong deformation of both parts of the cloud and a tendency of their separation from each other.

Evidently, in the 5–11 January 1997 events the magnetic cloud propagated in conditions close to those in the model for a cloud in a two-velocity stream. Actually it is

accepted widely that this cloud started on 6 January from the point with coordinates S23, W03 as part of the coronal mass ejection from the active filament in AO SN84 [*Webb et al.,* 1998]. The upper part of the cloud should have entered the southern part of the extensive roentgen coronal hole that was detected by *Watari and Watanabe* [1998], a low-latitude transient hole being observed in the hole on 8 January in the He 10830 line [*Burlaga et al.,* 1998].

Thus if the upper and low parts of the cloud were in the fast and slow streams of the solar wind, respectively, the *Schmidt and Cargill* [2001] model may be applied to the situation at least for a qualitative interpretation. One should however bear in mind that the reality might has been more complicated than this model because of a strong nonstationarity of the coronal hole and therefore a nonstationarity of the high-velocity stream.

Actually, the time sequence of the ejection (6 January) and the formation of a transient hole (8 January) are such that one can assume that the upper part of the cloud not only moved in the fast stream, but at some moment the velocity of this stream increased sharply, the fact not being taken into account in the model of a two-stream propagation of the cloud.

The distance (d) of the forward shock wave from the cloud magnetopause is an important characteristics which should be represented accurately in the modeling of a near-Earth disturbance. This distance depends on the cloud form and dimensions and the Mach number M of the incident stream. In the case considered here (a quasi-stationary motion of a cylinder with the radius $R_0 = 1.5 \times 10^{12}$ cm [*Burlaga et al.,* 1998] or $R_0 = 1.8 \times 10^{12}$ cm [*Hidalgo et al.,* 2000] in a stream with the magnetosonic number $M_{\rm ms} \approx M \approx 2$ [*Berdichevsky et al.,* 2000]) the value of d is of the order of $0.8\,R_0 \cong (1.2 \div 1.4) \times 10^{12}$ cm

[*Belotserkovsky*, 1957]. The observed value of d was found equal to

$$\sim V(t_{R1} - t_{sf}) \cos\varphi_N \approx 4.5 \times 10^7 \times 1.5 \times 10^4 \times 0.7 \cong 5 \times 10^{11} \text{ cm}$$

i.e. by more than a factor of two lower (V is the wind velocity, t_{R1}, t_{sf} are the observation moments of the cloud magnetopause and frontal wave, respectively).

Such strong discrepancy between the observed and theoretically expected values of d indicate to either a strong deviation of the cloud form from a round cylinder or to its strong acceleration already after the t_{sf} moment.

In the case of a super-expanded cloud in a two-velocity stream of the solar wind [*Schmidt and Cargill,* 2001] the shock wave may in principle be formed at any distance from the cloud magnetopause depending on the degree of its torsion and splitting into two sub-clouds.

Concluding this section, we once more would like to emphasize that one of the difficulties in modeling of the 6–11 January MHD-disturbance is the necessity to satisfy to the observed directions of normals (Table 3) and position of the frontal wave relative the cloud. Currently the cloud model in a two-stream solar wind [*Schmidt and Cargill*, 2001] with its further sophistication to the case of nonstationary streams seems perspective. We note also that *Odstrcil* [2001] reported preliminary results of the MHD-modeling of the 6–11 January 1997 disturbance at the Second European Conference on Solar Cycle and Space Weather. Contrary to the *Wu et al.* [1999] model, this model pays attention not only to the interaction of the cloud with the streamer but to the interaction of the high-velocity stream with the cloud in the scope of the concept of corotating interacting regions (CIR). From the computing point of view, it is an obvious complication of the model, since not only the large-scale irregularity of the interplanetary medium in front of SME but the solar rotation as well are taken into account. An applied potential of this approach (in particular, overcoming of the difficulties considered above) still remain

vague.

Thus the IMF components profiles obtained by sounding of magnetic clouds by near-Earth satellites in principle make it possible to formulate important limitations on configuration, structure, and dynamics of modeling disturbances. However since these profiles allow an ambiguous interpretation, they should be use carefully.

7.3. "Pulse" of the Proton Density on the Stream Interface

Unusually large increase of the solar wind proton concentration on the stream interface up to $n_{\max} \sim 185$ cm^{-3} [*Burlaga et al.,* 1998] (apparently the largest during the entire period of the near-Earth measurements of the density [*Fox et al.,* 1998]) is a specific characteristics of the 10–11 January 1997 interplanetary disturbance. There is no doubts that this increase indicates to some specific requirement to a MHD-modeling of this particular disturbance, since high densities on the stream interface were detected for the first time.

Various assumptions were made discussing this phenomenon. *Burlaga et al.* [1998] and *Reiner et al.* [1998] suggested that an increase by a factor of more than 30 (relative to the mean density) took place along the entire way from the Sun to the Earth. The increase was predetermined by the same densities in the solar filament and ambient corona. We should note that this fact was not taken into account in the MHD-modeling of this phenomenon by *Wu et al.* [1999]. *Safrankova et al.* [1998] and *Watari and Watanabe* [1998] assume that the density pulse might have appeared due to the interaction of the high-velocity stream from the coronal hole with the magnetic cloud. Apparently the presence of the dense substance of the protuberance at the rear wall of the cloud [*Burlaga et al.,* 1998] was one of important conditions of the occurrence of the density pulse, but it was hardly able to provide the high value of the pulse. However a quasi-stationary stream can not create such strong and sharp density changes on the stream interface,

this statement being confirmed both by the experiment and CIR theory [*Pizzo,* 1989; *Smith and Wolfe,* 1976]. If we accept the assumption made in Section 7.2 on a strong nonstationarity of the high-velocity stream (the fact being manifested in occurrence of the transient coronal hole in the He 10830 line), the "density pulse" becomes explained qualitatively within the framework of the super-expanding magnetic cloud model [*Cargill et al.,* 2000; *Schmidt and Cargill,* 2001]. Actually according to this model, entering of the cloud into the high-velocity stream (the velocity of which exceeds the magnetic cloud velocity at least by 15%, see Figures 6 and 7 in *Cargill et al.* [2000]) amplifies the cumulative effect at the rear wall of the super-expanding cloud and leads to a sharp increase of the particle density at this wall considerably exceeding the density increase in the front shock layer [Figure 7d in *Cargill et al.,* 2000]. Thus the unusually large density pulse may be explained by taking into account two factors: the presence of dense plasma of the protuberance [*Burlaga et al.,* 1998] and a cumulative effect at the rear wall of the cloud [*Cargill,* 2000].

This is one more requirement to the conditions of MHD-modeling of the 5–15 January 1997 disturbance.

7.4. Radiobursts of Type II: Indication to a Collision of the Nonstationary Stream With the Magnetic Cloud

The results of observations of the kilometer radiobursts of Type II [*Reiner et al.,* 1998] present an important indirect confirmation of the nonstationarity of the high-velocity stream and the generation of a "density pulse" as a result of the stream interaction with the magnetic cloud.

A narrow-band radioburst with a fast frequency drift in the ∼140–270 kHz range observed on 8 January (0400–1000 UT) present a special interest. Most likely, it is related

to the "density pulse" and have occurred at a distance of ∼0.38 AU from the Sun [*Reiner et al.,* 1998]. The radiation source had the angular dimensions of about 20°, was located slightly southward from the solar equator, and during the observations underwent a strong azimuthal displacement from 1.5°W to 7°W with a frequency decrease from 272 kHz to 148 kHz, respectively. This displacement corresponds to the velocity azimuthal component of about 500 km s^{-1}.

Reiner et al. [1998] underline that they could not suggest neither any rational mechanism of this emission nor explain such a fast azimuthal displacement of the radiation source. In principle, such emission might has been generated by the shock wave passing through the "density pulse." However, according to *Reiner et al.* [1998] this is unlikely, because there is no indications to a second shock wave in the data of the direct near-Earth measurements on board the Wind spacecraft [*Reiner et al.,* 1998].

If we accept the hypothesis on the interaction of a strongly nonstationary high-velocity stream from a transient coronal hole with the magnetic cloud, then the assumption on the second shock wave as a cause of the A-radioburst of type II [*Reiner et al.,* 1998] is completely acceptable for discussion. The absence of the second wave in the magnetic field and plasma measurements on board near-Earth satellites can be explained by the fact that the wave was short-lived and formed in the collisions of the fast stream with the back wall of the magnetic cloud. The shock wave rapidly ($V \geq 500$ km s^{-1}) and in an anisotropic way (strongly westward) propagating into the cloud, radiating in the corresponding radio wave range and strongly attenuating (for example, due to the growth of the magnetic sound velocity in the internal regions of the cloud), may be one of the consequences of such a collision. Having provided an additional compression and acceleration of the cloud, this wave might have disappeared long before approaching the Earth (see Section 7.7).

Thus the data on the kilometer radioburst of type II confirm indirectly the assumption on the interaction of a nonstationary stream with the magnetic cloud and these data should

be taken into account in MHD-modeling of the effects of this interaction.

In particular, one of possible effects of this interaction: the anomalous Forbush effect in the galactic cosmic rays (GCR) observed during the passage of the Earth through this disturbance [*Bieber and Evenson,* 1998] and apparently caused by a sudden significant compression of the cloud by the second shock wave (the MHD-pulse) formed in the cloud interaction with a nonstationary stream, is discussed in the following section.

7.5. Forbush Effect: A Confirmation of the Cloud Compression

In a broad sense, the Forbush effects are determined as changes of the density and anisotropy of the background cosmic rays (CR) caused by large-scale propagating disturbances of the solar wind [*Belov et al.,* 2001]. As a rule, a sequence of a forward shock wave and magnetic cloud leads to a two-stage decrease of the CR intensity.

However in the event in question, a decrease and increase of the intensity were observed in the shock wave and magnetic cloud, respectively [Figure 4 in *Bieber and Evenson*, 1998]. This is a rather rare modification of the Forbush effect which makes it possible to assume that there was a rapid compression of the cloud not long before its approaching the Earth [*Belov et al.,* 1999]. Thus the "anomaly" Forbush effect confirms a possibility of the cloud compression by the second shock wave generated during the running of the fast stream from the coronal hole against the rear cloud boundary (Section 7.4). Within the cloud the unit vector of the cosmic ray density gradient in the solar-ecliptic coordinate system (0.4; 0.3; -0.85) is parallel to the cloud boundary (perpendicular to the corresponding normal in Table 3), this fact adding an interesting detail to the general scenario of this disturbance.

It is worth noting also that *Bieber and Evenson* [1998] detected a CR anisotropy increase $\sim$40 hours prior to the arrival of the shock wave and interpreted this increase as

an indication to the earlier passage of the front part of this or any other CME southward from the Earth. This interpretation is of some interest for clarifying a possible role in this disturbance of the two earlier filament disappearances from the same AO AFSN84 region [*Webb et al.,* 1998]. Moreover, this region may be related to the preliminary development phase of the near-Earth disturbance started on 9 January 1997 [*Ivanov and Romashets*, 1997]. The normal to the forward front of this disturbance (RD_f) is shown in Table 3.

7.6. Growth Phase: Confirmation of the *Bieber and Evenson* [1998] Assumption

Three-phase temporal dynamics with the main and recovery growth phases is typical for the interplanetary disturbances near the heliospheric current sheet (HCS) called heliospheric substorms [*Ivanov et al.,* 1995]. It is assumed that the growth phase in the case of a filament–streamer disturbance (filament ejection in the vicinity of HCS) has a source the plasma escape from filament before the main ejection [*Ivanov et al.,* 1997]. The January disturbance may be such a substorm with the growth phase from ∼0600 UT on 9 January till the arrival of the shock wave front [*Ivanov and Romashets*, 1997]. The weaker and earlier sudden filament ejections from the same AO (0700–2300 UN on 5 January and 2119–1100 UT on 5–6 January) preceding to main ejection at 1301–1453 UT could be a solar source of this phase [*Webb et al.,* 1998].

Usually a growth phase begins by a strong front rupture and presents monotone variations of the average IMP modulated by nonlinear Alfvén waves and fractures [*Ivanov and Petrov*, 1999]. Similar variations were observed in this case (Figures 11 and 12). Table 3 shows the normal to the front rotating fracture RD_f. The following oscillations propagated in this direction ($\varphi_N = 160°$, $\theta_N = 10°$) from the south-west to the north-east.

In connection to this, the southern anisotropy in the GCR density distribution, which

appeared ∼40 hours prior to the shock wave front arrival and was an indirect indication to one more CME passing southward from the Earth [*Bieber and Evenson*, 1998], may be related to the growth phase observed during this time [*Ivanov and Romashets*, 1997].

Figures 11 and 12 show variations of the IMF B, B_X, B_Y, and B_Z components and the V_x, V_y, and V_z components of the solar wind velocity measured on board the Wind satellite at the growth phase. These variations were compared to the moments of the southern anisotropy maxima taken from *Bieber and Evenson* [1998].

These variations are expressive enough: (1) $V_Z > 0$ during the whole phase, V_y varies smoothly with a sign change near the anisotropy maximum (this fact indicates on the whole to a clearly pronounced northward motion (expansion) component of the southern source; (2) the IMF B_x component decreases monotonically almost to zero near the anisotropy maximum, after that undergoes sharp direction changes, and finally restores the previous direction; the B_Z component changes its direction from the southward to northward at the end of the growth phase. Such B_x and B_y variations indicate to the IMF draping of the positive sector near the upper part of some obstacle southward from the Earth.

Thus the direct measurements of the magnetic field and plasma on board satellites and at ground-based monitors observing the GCR anisotropy during the growth phase, make it possible to put forward a coordinated assumption that before the main SME responsible for the shock wave and magnetic cloud on 10–11 January, one more CME propagated in the interplanetary medium southward from the Earth helioprojection and caused the above-described fine features of the variations of the IMF, solar wind plasma, and GCR anisotropy on 9 January at the growth phase of this disturbance.

Certainly, the interplanetary medium properties on 9 January should be taken into account in a detailed modeling of the 10–11 January 1997 disturbance. In particular one should bear in mind that the nonlinear fluctuations of the IMF at the growth phase are

amplified in the front shock layer, make the intermediate CME region very inhomogeneous, make the identification of the magnetic cloud magnetopause difficult, and (as it occurs in this case (Figure 13)) initiate various assumptions on their nature [*Farrugia et al.,* 1998; *Tsurutani et al.*, 1998].

7.7. MHD-Structure of the Cloud Vicinities. The Velocity Field in the Flowing-Around Region and Within the Cloud

Figure 14 shows the variations of the plasma parameters n, V_x, V_y, V_z, and V_{th} obtained during the passage of the Wind satellite through the magnetic cloud and its vicinities. The cloud itself and the front and rear thickening jumps are shown.

The front cloud boundary (magnetopause) is shown at ∼0500 UT on 10 January (denoted as R_1) in agreement with the *Burlaga et al.* [1998] determination, although *Farrugia et al.* [1998] and *Hidalgo et al.* [2000] proposed to transfer the time of the entrance into the cloud from 0500 UT to 0700 UT, this transfer making possible to choose smoother profiles of the IMF components in the inverse problem of this cloud modeling. In a more detailed consideration of the magnetopause, it is desirable to take into account the presence of a wide boundary layer at ∼0430–0700 UT embracing magnetopause. Part of this layer (0439–0458 UT) is identified presumably with one of the external CME loops connected to the magnetopause [*Tsurutani et al.,* 1998] or with a "plasma depletion layer" [*Farrugia et al.,* 1998]. Such boundary layers have already been observed in the past [*Ivanov,* 1984; *Ivanov and Fel'dshtein*, 1982]. They indicate to a complex character of the interaction with a reconnection of the magnetic fields at the cloud front boundary and (as it becomes clear now [*Poedts,* 2001]) require a careful allowance for in the process of MHD modeling.

To determine the cloud rear boundary is even a more difficult problem. One of

possibilities is to identify it with the "magnetic hole" (MH) [*Burlaga et al.,* 1998] which seems fully acceptable in our view. The accurate position of the stream interface SI remains unclear. *Burlaga et al.* [1998] determined the SI passing time as ∼0700 UT on 11 January. The IMF and plasma variations at this time allow an assumption on the front of the nonlinear fast shock wave S_r propagating sunward. If we identify the stream interface with the "magnetic hole," the assumption that the stream interface of this disturbance is an interplanetary continuation of the intersector boundary (Section 4) would make it possible to consider namely the "magnetic hole" as a specific property of the boundary between the two giant tubes of open lines coming from different parts of the photosphere.

The velocity field in the front and rear thickening jumps seems to be very complex and excludes simple interpretation in terms of a hydrodynamic flowing around without a special study.

Within the cloud the V variations are more regular (*Burlaga et al.* [1998] paid attention to the cloud motion as a whole with a velocity of ∼15 km s^{-1} southward) and deserves a special attention in relation to the assumption on an appearance and dissipation of the second shock wave responsible for the kilometer radioburst of type II (Section 7.4). It is worth reminding that *Reiner et al.* [1998] emphasized that the A-type radioburst with a rapid frequency drift observed on 8 January may be explained by a passage of one more shock wave. We suggested that such a wave might have aroused due to the interaction of the nonstationary stream from the coronal hole to the rear wall of the magnetic cloud. Further on propagating within the cloud, the wave becomes gradually weaker. The sharp enough velocity jump from $V_1(-440; 20; -10)$ km s^{-1} to $V_2(-460; 0; -45)$ km s^{-1} observed on board the Wind satellite (Figure 14) approximately at 1200 UT on 10 January (F) presents apparently the very nonlinear MHD wave to which this shock wave front has degenerated. The front F is located closer to the front boundary of the cloud and since the momentum of its assumed generation (∼0500 UT on 8 January 1997 [*Reiner et al.,*

1998]) it must have passed from the rear cloud wall a path equal to $\sim 2.4 \times 10^{12}$ cm with the average velocity of $\sim$120 km s^{-1} close to the Alfvén velocity in the cloud ($\sim$110 km s^{-1} in the moment the front passage).

It is interesting that the moment of the front F arrival may be interpreted as a cloud acceleration in the radial and south-eastern directions, the velocity jump vector $\Delta V = (-20; -20; -35)$ being directed along $\varphi_{\Delta V} = 225°, \theta_{\Delta V} = -40°$. This direction coincides with the directions of normals to the main structure boundaries of this disturbance (Section 7.1, Table 3).

8. Discussion

It is assumed that as a result of large-scale hydrodynamic interactions in the convective zone of the Sun which were manifested in the displacements and mutual convergences of four photospheric regions of open lines (OR) (Figure 1, Table 1), at the 9 January rotation there was formed on the considered part of the solar disk an unstable configuration of the solar magnetoplasma with a free energy excess.

The nonequilibrium substructure of the coronal magnetic field with a strong deflection of sector boundary formed by the open lines from the near-equatorial photosphere and southern polar cap and a strongly unstable intersector boundary between the open near-equatorial and polar lines of the positive sector was a manifestation of this unstable zone at the boundary with the interplanetary medium (on the stream interface). The "joint" between the above-indicated sector and intersector boundaries and the boundary of the small subsector of open lines of the southern polar zone was the most nonequilibrium element of this structure.

A low-atmosphere manifestation of this free energy zone was a complex consisting of: (1) AO SN84 with active filaments distributed under the "joint" of above-indicated

subsector boundaries; (2) the roentgen coronal hole filling in the near-equatorial region of positive open lines; (3) AO 8009 with the magnetic stream which has just went to the surface.

To simulate solar-terrestrial relations one needs ideas on the dynamics, structure, and configuration of this free energy zone before, during, and as a result of its destabilization. This would make it possible to formulate the initial conditions for solving the MHD-equations describing CME ejections and their propagation through the interplanetary medium. It is also clear that in principle each out of the above-indicated elements of the photospheric–coronal activity complex, as well as the characteristics of the field substructure on the source surface, pay a role in the CME formation and exit into the interplanetary medium. Resuming, one can formulate some conditions which should be fulfilled in MHD-modeling of these disturbances.

In the concept of a complex interplanetary disturbance from a complex source [*Burlaga et al.,* 1987; *Bravo et al.,* 1998; *Crooker and McAlister*, 1997; *Dryer,* 1974; *Gonzalez et al.,* 1996; *Ivanov,* 1996, 1998; *Mogilevsky et al.,* 1997] the complex source may be a combination of independent (i.e. noninteracting with each other on the Sun [*Dryer,* 1974]) phenomena, or a sequence of phenomena partially or entirely related by the interaction in unstable large-scale structure of the free energy zone [*Gosling*, 1993]. These two concepts are used usually to define ideas on the sources in each particular solar disturbance. The variability there is strong and the development level of these ideas is insufficient.

The 1–15 January 1997 solar-terrestrial disturbance is undoubtedly relatively simple. Nevertheless at our glance, there are neither ideas on its complex source sufficient to put correct initial conditions for simulation, nor information on its near-Earth interplanetary manifestation sufficient for absolutely complete testing of the models. Some of the qualitative scenario of this disturbance developed in the previous papers may be completed by

the above-mentioned results.

First, a sequence of three DSF ejected on 5–6 January from AO SN84 (only the third ejection (1301–1453 UT on 6 January) was registered as a coronal CME by the LASCO/SOHO device [*Bruckner et al.,* 1998; *Burlaga et al.,* 1998; *Webb et al.,* 1998]) was observed in the interplanetary medium as sequence of three CME (Section 7.6), the disturbances from two first (weaker) CME being observed as effects in the GCR anisotropy variations [*Bieber and Evenson,* 1998] and in the specific variations of the IMF and solar wind plasma. These two first CME propagated directly before the third one (which aroused the strongest interest) and were able to influence its propagation, the fact being worth taking into account in the modeling.

Second, very low intensity of the LDE (long duration event) phenomenon in roentgen after the main CME ejection was observed [*Webb et al.,* 1998]. This fact apparently indicates to the glow carrier distribution over very large volume of the magnetic tubes [*Hudson et al.,* 1998]. It is worth drawing attention to the fact that the filament started near the sector boundary formed by the near-equatorial and polar lines (Figure 2) and therefore the posteruptive arcade formed by these lines may have a rather large volume. Thus one can assume that in this disturbance one of CME modifications possible for a year of solar minimum was observed on magnetic tubes connecting the opposite hemispheres [*Kahler,* 1991].

One can match to such CME modification also formation in the vicinity of this AO of only one northern "dimming" (coronal dimness) on the place of a part of the bright roentgen arc crossing the filament [*Webb et al.,* 1998] and apparently going into the near-equatorial photosphere northward from HCS. Another "dimming" may be located in the polar regions of the Southern hemisphere at the negative lines of the OR-2 region (Figure 1). In this case, there may be a solution of one of enigmatic problems on the physical sense of a partially asymmetric halo during a CME passage through the corona

[*Burlaga et al.*, 1998]. Actually if this halo is a result of the coronal substance ejection from the tubes adjacent to the high-velocity magnetic cloud, then in this event the adjacent tubes northward from the CME are near-equatorial and southward from the CME are high-latitudinal (subsector OR-2 in Figure 2), the latter having photospheric "roots" in the polar zone south-westward from the filament ejection place.

Third, the assumption on the compression of the magnetic cloud by the high-velocity corotating stream from the coronal hole located northward from the CME starting place [*Burlaga et al.,* 1998; *Watari and Watanabe,* 1998] leads naturally to a concept of super-expanding cloud motion in the two-velocity solar wind (Section 7.2). In this case, the use of the motion model of this cloud [*Cargill et al.*, 2000; *Schmidt and Cargill*, 2001] leads to various consequences which agree qualitatively to various observations: 1) the complex flattened and twisted form of the cloud with a small shift of the forward shock wave from the magnetopause (Sections 7.1–7.2); 2) the formation of a "density pulse" at the cloud rear boundary (Section 7.3); 3) a necessity to model the cloud magnetic field, taking into account the boundary currents on the cloud magnetopause (Section 7.2); 4) the formation and attenuation of the second shock wave at the cloud rear boundary according to the data on kilometer radiobursts of type II (Section 7.4); 4) the strong compression of the cloud (up to an occurrence of an anomaly Forbush-effect: Section 7.5) and its acceleration in the south-western direction (Section 7.7).

Fourth, the assumption on the stream interface (SI) as an interplanetary manifestation of the intersector boundary [*Ivanov et al.,* 2001a] is confirmed. This is the first case since the introduction of a SI term [*Burlaga et al.,* 1974] when such interface is connected with a well determined boundary in the coronal magnetic field which have a clear MHD interpretation as a boundary between individual photospheric regions of the open lines of the same polarity. It is also worth noting that in this particular case SI is very close to the rear wall of the magnetic cloud, i.e. to the "magnetic hole" MH [*Burlaga*

et al., 1998]. The latter fact should be taken into account in the MHD modeling of this disturbance. However there arises a difficulty in matching to the time of appearance of the low-latitude coronal hole in the He 10830 emission (for the first time this hole was registered on 8 January in 2043 UT [*Burlaga et al.,* 1998]), since we suppose that the strong nonstationary of the high-velocity stream needed to compress the magnetic cloud should have occurred much earlier, in the beginning of 8 January (Sections 7.3–7.4). This problem is still obscure. It is possible that there are circumstances due to which the high-velocity stream from OR +3 accelerated earlier than in the front part of this region there appeared the indication to the nonstationarity of the corresponding coronal hole in the form of the He 10830 A line emission. Carrying along of the plasma by the magnetic cloud from the adjacent open tubes coming from the corresponding near-equatorial part of the photosphere may be such a circumstance.

Fifth, the common ideas on magnetic twists and the heliographic dependence of their spirality [*Bothmer and Schwenn*, 1998; *Forbes*, 2000; *Marubashi*, 1986] used in the analysis of this disturbance [*Burlaga et al.,* 1998; *Wu et al.,* 1999] find their confirmation. Moreover it is shown (apparently for the first time) that a magnetic cloud may contain in its tail part the protuberance substance [*Burlaga et al.,* 1998]. At the same time, it was found that, solving the inverse problem of finding the cloud geometric characteristics form the IMF component profiles, the use of the powerless cylinder cloud model (which proved its applicability in many other cases [*Burlaga*, 1988]) in this case leads to contradictions to the observed directions of the normals. A sophistication of the model is needed by taking into account of the boundary currents and a complex form of the cloud.

The most difficult is the problem of the role of various solar activity phenomena and their interaction with each other at the stage of generation of the large-scale unstable structure, its destabilization, and coming out of the corresponding CME into the interplanetary medium. In the solar physics this problem is split to a series of peculiar

problems, for example: an interaction of coronal holes with active regions [*Adams,* 1976; *Mogilevsky and Shilova*, 1995; *Sheeley et al.,* 1989; *Vorpahl and Broussard*, 1978], or interaction of active regions with each other [*Kahler*, 1991]. To explicitly formulate the initial conditions for the MHD modeling of CME, it is desirable to have information on all such interactions. Even in the relatively simple event on 5–6 January 1997 it would be desirable to know all essential things not only about the coming out of active filaments from AO SN84, but about the interaction of this AO and corresponding CME with the coronal hole and heliospheric current layer, and possible with AO 8009 which (within the concept of connected AO [*Kahler,* 1991]) might have input to the CME generation.

9. Conclusion

To model successfully solar-terrestrial physics phenomena, the following ideas should be developed:

1) the ideas on the structure, configuration, and dynamics of complex solar sources of near-Earth disturbances; this would make it possible to put explicitly enough the initial conditions for the MHD equations system describing the disturbance propagation from the Sun to Earth;

2) the ideas on the structure, configuration, and dynamics of complex near-Earth disturbances which would make it possible to test reliably MHD-models of these disturbances.

To solve these problems, it would be desirable to develop the studies in which the synoptic analysis of the data on prominent events presents a combination of two approaches complimenting each other: 1) a more broad (than it is common now) coverage of the phenomena beginning from the dynamics of the photospheric regions of open lines and up to near-Earth disturbances; 2) attraction (together with the data of direct measurements)

also of significant indirect data which currently are not used completely.

An attempt is made in this paper to analyze in the above-indicated way the data on a prominent event on 5–11 January 1997 which initiated a large number of publications on various aspects of this disturbance.

The analysis performed makes it possible to draw the following conclusions:

(1) The solar data does not contradict the suggestion that the slow convergence of several large-scale photospheric regions of open lines with a characteristic time on the order of one solar rotation initiated a large-scale unstable configuration of the coronal magnetic field and the related complex of solar activity phenomena, the latter becoming a cause of the solar-terrestrial event on 5–11 January 1997.

(2) The "joint" between the sector and intersector boundaries was a feature of the large-scale configuration of the coronal field. The joint boundaries were formed by the open lines coming onto the source surface from the near-equatorial and polar photospheric regions remote from each other. One of the polar regions was shifted considerably south-westward from the central meridian, the latter fact possibly predetermining the configuration of the partial halo of the corresponding CME (a south-westward shift with the axis at a positional angle of 50 W).

(3) Under the joint there was a filament-active region AO. A sequence of three suddenly disappearing filaments from this AO became one of the causes of the coronal-interplanetary disturbance on 5–11 January 1997.

(4) The first two weak filament ejections propagated outside the heliospheric streamer in front of the main CAO. Their passage southward from the Earth was registered at the development phase of the 8–9 January near-Earth event on the basis of the variations of the GCR anisotropy vector and specific variations of the IMF and solar wind plasma.

(5) The high-velocity stream from the nonstationary hole formed at the intersector boundary in the vicinity of the Earth helioprojection and its running against the CME

magnetic cloud were able to lead to some effects which follow from the model of a super-expanding cloud in a two-velocity solar wind [*Cargill et al.,* 2000; *Schmidt and Cargill*, 2001]. The effects include, in particular:

a) a strong compression and deformation of the cloud; b) a formation of a "density pulse" due to a cumulative effect at the cloud rear wall; c) a generation and then attenuating of a second shock wave responsible for the observed kilometer radioburst of type II with a fast frequency drift; d) an anomalous Forbush effect; e) a development of strong boundary currents which determined considerably the IMP component profiles within the cloud.

Acknowledgments. The authors thank R. Lepping, R. Ogilvie, and the CDAWeb Group for the data of the magnetic field and plasma measurements on board the Wind satellite, T. Hoeksema for the data of the photospheric field measurements on board WSO, and A. I. Zavoikina for her help in the preparation of the paper. The work was supported by EU/INTASS-ESA (grant No. 99-00-727), Russian Foundation for Basic Researches (project No. 00-05-64259) and the Russian Foundation for the "Astronomia" Program.

References

Adams, W. M., Differential rotation of photospheric magnetic fields associated with coronal holes, *Sol. Phys., 47*(2), 601, 1976.

Belov, A. V., V. A. Oleneva, and V. G. Yanke, Transient effects in cosmic rays during 1980–1995, *Izv. Ros. Akad. Nauk, Ser. Fiz. (in Russian), 63*(8), 1634, 1999.

Belov, A. V., et al., That causes Forbush effects and that they are related to?, *Izv. Ros. Akad. Nauk, Ser. Fiz. (in Russian), 65*(3), 373, 2001.

Belotserkovsky, O. M., Flowing around of a circular cylinder with the bow shock wave, *Dokl. Akad. Nauk SSSR (in Russian), 113*(3), 509, 1957.

Berdichevsky, D. B., A. Sabo, R. P. Vinas, and F. Mariani, Interplanetary fast shocks and associated drivers observed through the 23th solar minimum by Wind over its first 2.5 years, *J. Geophys. Res., 105*(A12), 27,289, 2000.

Bieber, J. W., and P. Evenson, Coronal mass ejection geometry in relation to cosmic ray anisotropy, *Geophys. Res. Lett., 25*(15), 2955, 1998.

Bothmer, V., and R. Schwenn, The structure and origin of magnetic clouds in the solar wind, *Ann. Geophys., 16*(1), 1, 1998.

Bravo, S., X. Blanco-Cano, and E. Nikiforova, Different types of coronal mass ejections at minimum and maximum of solar activity and their relation to magnetic field evolution, *Sol. Phys., 180*(1/2), 461, 1998.

Bruckner, G. E., et al., Geomagnetic storms caused by coronal mass ejections: March 1996 through June 1997, *Geophys. Res. Lett., 25*(15), 3019, 1998.

Bumba, V., Does the large-scale solar magnetic field distribution really reflect the convective velocity fields?, *Sol. Phys., 110*(1), 51, 1987.

Bumba, V., and R. Howard, Large-scale distribution of solar magnetic fields, *Astrophys. J., 141*(4), 1502, 1965.

Burlaga, L. F., Interplanetary stream interfaces, *J. Geophys. Res., 79*, 3717, 1974.

Burlaga, L. F., Magnetic clouds, and force-free fields with constant alpha, *J. Geophys. Res., 93,* 7217, 1988.

Burlaga, L. F., K. W. Behannon, and L. W. Klein, Compound streams, magnetic clouds, and major magnetic storms, *J. Geophys. Res., 92*, 5725, 1987.

Burlaga, L. F., et al., A magnetic cloud containing prominence material: January 1997, *J. Geophys. Res., 103*(1), 277, 1998.

Canfield, R. C., H. S. Hudson, and D. E. McKenzi, Sigmoidal morphology and eruptive solar activity, *Geophys. Res. Lett., 26*(6), 627, 1999.

Cargill, P. J., J. Schmidt, D. S. Spicer, and S. T. Zalezhak, Magnetic structure of over-

expanding coronal mass ejections. Numerical models, *J. Geophys. Res., 105,* 7509, 2000.

Cid, C., et al., Evidence of magnetic flux ropes in the solar wind from sigmoidal and non-sigmoidal active regions, *Sol. Phys., 198*(1), 169, 2001.

Crooker, N. U., and A. N. McAlister, Transients associated with recurrent storms, *J. Geophys. Res., 102*(A7), 14,041, 1997.

Dryer, M., Interplanetary shock waves generated by solar flares, *Space Sci. Rev., 15*(4), 403, 1974.

Dryer, M., Comments on the "Solar flare myth" paradigm, in *Proceedings of Second SOLTIP Symposium*, p. 181, 1995.

Dryer, M., and Z. K. Smith, MHD simulation of multiple interplanetary disturbances during STIP interval VII (August 1979), in *Solar Maximum Analysis*, edited by V. E. Stepanov and V. N. Obridko, p. 369, VNU Science Press, Utrecht, 1987.

Farrugia, C. J., et al., Unusual features of the January 1997 magnetic cloud and their effect on optical dayside aurora signatures, *Geophys. Res. Lett., 25*(15), 3051, 1998.

Forbes, T. G., A review on the genesis of coronal mass ejections, *J. Geophys. Res., 105*(A10), 23,153, 2000.

Forbes, T. G., and E. R. Priest, Photospheric magnetic field evolution and eruptive flares, *Astrophys. J., 446*, 377, 1995.

Fox, N. J., M. Peredo, and B. J. Thompson, Cradle to Grave traking of the January 6–11, 1997 Sun–Earth connection event, *Geophys. Res. Lett., 25*(14), 2461, 1998.

Funsten, H. O., et al., Combined Ulusses solar wind and SOHO coronal observations of several west limb CMEs, *J. Geophys. Res., 104*(A4), 6679, 1999.

Gonzalez, W. D., et al., Coronal hole–active region–current sheet (CHARCS) association with intense interplanetary and geomagnetic storms, *Geophys. Res. Lett., 23*(19), 2577, 1996.

Gosling, J. T., The solar flare myth, *J. Geophys. Res., 98*, 18,937, 1993.

Hidalgo, M. A., C. Cid, J. Medina, and A. F. Vinas, A new model for the topology of magnetic clouds in the solar wind, *Sol. Phys., 194*(1), 165, 2000.

Hudson, H. S., J. R. Lemen, O. C. St. Cyr, A. C. Sterling, and D. F. Webb, X ray coronal changes during halo coronal mass ejections, *Geophys. Res. Lett., 25*(14), 2481, 1998.

Ivanov, K. G., Specification of the phenomenological model of the interplanetary flare stream: the slow wave and boundary layer, *Geomagn. Aeron. (in Russian), 24*(1), 22, 1984.

Ivanov, K. G., Solar sources of the interplanetary plasma streams at the Earth's orbit, *Geomagn. Aeron. (in Russian), 36*(2), 19, 1996.

Ivanov, K. G., Solar sources of interplanetary plasma streams at Earth's orbit, *Int. J. Geomagn. Aeron., 1*(1), 1, 1998.

Ivanov, K. G., Arc filament systems as solar sources of the near-Earth disturbances, *Geomagn. Aeron. (in Russian), 40*(1), 3, 2000.

Ivanov, K. G., and Ya. I. Fel'dshtein, On detection of boundary layers in the interplanetary magnetoplasma, *Geomagn. Aeron. (in Russian), 22*(4), 672, 1982.

Ivanov, K. G., and A. F. Kharshiladze, Slow dynamics of the open field lines as an indicator of subphotospheric interactions, its relation to solar activity phenomena and near-Earth disturbances. 2. The March–September 1999 events, *Geomagn. Aeron. (in Russian), 42*(2), 2002 (in press).

Ivanov, K. G., and V. G. Petrov, The MHD structure of the precursors of interplanetary and geomagnetic disturbances in the vicinity of the heliospheric current sheet, *Geomagn. Aeron. (in Russian), 39*(4), 3, 1999.

Ivanov, K. G., and E. P. Romashets, January 5–12, 1997 heliospheric substorm: morphology and interpretation, *Bull. Am. Astron. Soc., 29*(2), 905, 1997.

Ivanov, K. G., and E. P. Romashets, Heliospheric current sheet effect on propagation of

type II interplanetary radio bursts from coronal mass ejections, *Radio Sci., 36*(6), 1739, 2001.

Ivanov, K. G., V. A. Styazkhin, E. U. Eroshenko, and E. P. Romashets, Twin Phobes 1 and Phobes 2 observations of heliospheric disturbances near the heliospheric current sheet, in *Solar Wind Eight,* edited by D. Winterhalter and J. T. Gosling, p. 575, AIP Press, 1995.

Ivanov, K. G., et al., Heliospheric substorm on November 26–December 5, 1977, 1, Solar sources, growth phase, and shock waves, *Geomagn. Aeron. (in Russian), 37*(2), 18, 1997.

Ivanov, K. G., V. Bothmer, P. Cargill, A. F. Kharshiladze, E. P. Romashets, and I. S. Veselovsky, Subsector structure of the interplanetary space, *Program and Abstracts of Euroconference Solar Cycle and Space Weather*, p. 35, Vico Equense, Italy, 2001a.

Ivanov, K. G., A. F. Kharshiladze, and A. N. Mel'nik, Slow dynamics of the open field lines as an indicator of subphotospheric interactions, its relation to solar activity phenomena and near-Earth disturbances. 1. The July–October 1999 events, *Geomagn. Aeron. (in Russian), 41*(6), 1, 2001b.

Kahler, S., Coronal mass ejections and streamers associated with the new cycle activity regions at solar minimum, *Astrophys. J., 378*, 398, 1991.

Kaiser, M. L., et al., Type II radio emission in the frequency range from 1 to 14 MHz associated with the April 7, 1997 solar event, *Geophys. Res. Lett., 25*(14), 2501, 1998.

Kharshiladze, A. F., and K. G. Ivanov, Spherical harmonic analysis of the solar magnetic field, *Geomagn. Aeron. (in Russian), 34*(4), 22, 1994.

Levine, R. H., M. D. Altschuler, and J. W. Harley, Solar sources of interplanetary magnetic field and solar wind, *J. Geophys. Res., 82,* 1061, 1977.

Lewis, D. J., and J. M. Simnett, The occurrences of coronal mass ejections at solar minimum and their association with surface activity, *Sol. Phys., 191*(1), 185, 2000.

Marubashi, K., Structure of the interplanetary magnetic clouds and their solar origins, *Adv. Space Res., 6*(6), 33, 1986.

Mogilevskiy, E. I., and N. S. Shilova, Disintegration of solar H-α filaments and recurrent geomagnetic disturbances, *Geomagn. Aeron. (in Russian), 36*(5), 43, 1996.

Mogilevsky, E. T., V. N. Obridko, and B. D. Shelting, Large-scale magnetic field structures and coronal holes on the Sun, *Sol. Phys., 176*(1), 107, 1997.

Odstrcil, D., Numerical simulation of 3-D interplanetary disturbances, *Program and Abstracts Euroconference Solar Cycle and Space Weather*, p. 33, Vico Equense, Italy, 2001.

Odstrcil, D., and V. J. Pizzo, Three dimensional propagation of coronal mass ejections (CMEs) in a structured solar wind flow, 1, CME launched within the streamer belt, *J. Geophys. Res., 104*, 483, 1999.

Ogilvie, K. W., R. Fitzenreiter, and M. Desh, Electrons in the low density solar wind, *J. Geophys. Res., 105*(A12), 27,277, 2000.

Pizzo, V. G., The evolution of corotating stream fronts near the elliptic plane in the inner solar system. 1. Two-dimensional fronts, *J. Geophys. Res., 94*(7), 8673, 1989.

Poedts, S., Numerical modeling of CME initiation and propagation, *Program and Abstracts of Euroconference Solar Cycle and Space Weather,* p. 28, Vico Equense, Italy, 2001.

Reiner, M. J., M. L. Kaiser, J. Fainberg, J.-L. Bougeret, and R. J. Stone, On the origin of radio emission associated with January 6–11, 1977 CME, *Geophys. Res. Lett., 25*(14), 2493, 1998.

Riley, P., J. T. Gosling, and V. J. Pizzo, A two dimensional simulation of the radial and latitudinal evolution of a solar wind disturbance driven by a fast, high pressure coronal mass ejection, *J. Geophys. Res., 102*, 14,677, 1997.

Safrankova, J., et al., The January 10–11, 1997, magnetic cloud: Multipoint measurements, *Geophys. Res. Lett., 25*(14), 2549, 1998.

Schmidt, J., and P. J. Cargill, Magnetic cloud evolution in two-speed solar wind, *J. Geophys. Res., 106*(4), 8283, 2001.

Sheeley, N. R., Y.-M. Wang, and J. W. Harvey, The effect of newly erupting flux on the polar coronal holes, *Sol. Phys., 119*(2), 323, 1989.

Sheeley, N. R., J. H. Walters, Y.-M. Wang, and R. A. Howard, Continuous tracking of coronal outflows: two kinds of coronal mass ejections, *J. Geophys. Res., 104*(A11), 24,739, 1999.

Shodhan, S., et al., Counterstreaming electrons in magnetic clouds, *J. Geophys. Res., 105*(A12), 27,261, 2000.

Smith, E. J., and J. H. Wolfe, Observations of interaction regions and corotating shocks between one and five AU, *Geophys. Res. Lett., 3*(2), 137, 1976.

Starr, V. P., and H. J. Fisher, Active regions and the large-scale flow in the solar photosphere, *Pure Appl. Geophys., 92*(9), 219, 1971.

Subranian, P., K. P. Dere, N. B. Rich, and R. A. Howard, The relationship of coronal mass ejections to streamers, *J. Geophys. Res., 104*(A10), 22,321, 1999.

Tsurutani, B. T., et al., The January 10, 1997 auroral hot spot horseshoe aurora and first substorm: A coronal mass ejection loop?, *Geophys. Res. Lett., 25*(15), 3047, 1998.

Vorpahl, J. A., and R. U. Broussard, Physical parameters defining the changing structure of a coronal hole, *Astrophys. J., 300*(1), 219, 1978.

Ward, F., General circulation of the solar atmosphere from observational evidence, *Pure Appl. Geophys., 58*(1), 157, 1964.

Ward, F., The general circulation of the solar atmosphere and maintenance of the equatorial acceleration, *Astrophys. J., 141*(2), 534, 1965.

Watari, S., and T. Watanabe, The solar drivers of geomagnetic disturbances during solar minimum, *Geophys. Res. Lett., 25*(14), 2489, 1998.

Webb, D. F., E. W. Cliver, N. Gopalswamy, H. S. Hudson, and O. C. St. Cyr, The solar

origin of the January 1997 coronal mass ejection, magnetic cloud, and geomagnetic storm, *Geophys. Res. Lett., 25*(14), 2469, 1998.

Wu, S. T., W. P. Guo, D. J. Michels, and L. F. Burlaga, MHD description of the dynamical relationships between a flux rope streamer, CME, and magnetic cloud: An analysis of the January 1997 Sun–Earth connection event, *J. Geophys. Res., 104*(A7), 14,789, 1999.

Zhao, X. P., and J. T. Hoeksema, Is the geoeffectiveness of the 6 January 1997 CME predictable from solar observations, *Geophys. Res. Lett., 24*(23), 2965, 1997.

V. Bothmer, Max-Plank Institut für Aeronomie, Katlenburg-Lindau, Germany.

P. J. Cargill, Imperial College of Science, Technology, and Medicine, London, UK.

K. G. Ivanov, A. F. Kharshiladze, and E. P. Romashets, Institute of Terrestrial Magnetism, Ionosphere, and Radio Wave Propagation, Troitsk, Moscow Region, Russia.

I. S. Veselovsky, Moscow State University, Russia.

(Received 10 December 2001)

Table 1. Distance r Between the Photospheric Regions of Open Lines (OR); C and R Are the OR Mutual Convergence or Divergence

13 December 1996		9 January 1997			5 February 1997		
OR	r, R_0	OR	r, R_0	C, R	OR	R, R_0	C, R
$+1/-1$	1.88	$+1^*/-1$	1.92	R	$+1^*/-1$	1.94	R
$+1/-2$	1.84	$+1^*/-2$	1.76	C	$+1^*/-2$	1.82	R
$+1/+1$	0.7	–	–	C	–	–	–
$+2/+3$	0.92	$+1^*/+3$	1.26	R	$+1^*/+3$	1.01	C
$+2/-2$	1.85	–	–	–	$+1^*/-3$	1.69	R
$+2/-3$	1.28	$+1^*/-3^*$	1.47	R	$+3/-2$	1.34	R
$+3/-2$	1.39	$+3/-2$	1.18	C	$+3/-3^*$	1.26	R
$+3/-3$	1.22	$+3/-3^*$	0.92	C			
$-3/-4$	0.6	–	–	C	$+1/-1$a	1.77	–

Table 2. Sector (HCS) and Intersector (SB) Boundaries of the Coronal Magnetic Field for Three Solar Orbits Centered at 13 December 1996, 9 January 1997, and 5 February 1997

13 December 1996		9 January 1997		5 February 1997	
4 December	HCS $(-0/+1)$	31 December	HCS $(-0/+1^*)$	30 January	HCS $(-0/+1^*)$
8 December	SB$(-1/+0)$	2 January	SB$(+1^*/+1^*$a$)$	31 January	SB$(1^*/+1^*$a$)$
9 December	SB$(+0/+2)$	5 January	SB$(1^*$a$/1^*)$		
10 December	SB$(+2/+3)$	7 January	SB$(1^*/+3)$	3 February	SB$(1^*$a$/+3)$
14 December	HCS$(+3/-3)$	11 January	HCS$(+3/-3^*)$	7 February	HCS$(+3/-3^*)$
18 December	SB$(-3/-4)$	15 January	SB$(-3^*/-0)$	11 February	SB$(-3^*/?)$

Table 3. Normals to the Boundaries

Data	UT	Boundary	φ_n, deg	θ_N, deg	Source
10 January 1997	0051	S_f	212		[*Safrankova et al.,* 1998]
10 January 1997	0051	S_f	200	-30	[*Berdichevsky et al.,* 2000]
10 January 1997	0051	S_f	205	-19	This paper
10 January 1997	0205	TD_1	194	-25	[*Tsurutani et al.*, 1998]
10 January 1997	0252	TD_2	218	-30	[*Tsurutani et al.*, 1998]
10 January 1997	0441	TD_3	205	-30	[*Tsurutani et al.*, 1998]
10 January 1997	0459	TD_4	205	-30	[*Tsurutani et al.*, 1998]
10 January 1997	0442	R_1	214	-17	This paper
11 January 1997	∼0100	SI_1	212		[*Safrankova et al.,* 1998]
11 January 1997	∼0200	SI_2	228		[*Safrankova et al.,* 1998]
11 January 1997	∼0300	MH	198	-33	This paper
9 January 1997	0930	RD_f	160	10	This paper

Table 4. The Magnetic Cloud Parameters

φ_a, deg	θ_a, deg	R_0, cm	R_0, cm	φ_n, deg	θ_N, deg	Source
250	03	1.5×10^{12}	0.2×10^{12}	160	8	[*Burlaga et al.,* 1998]
259	06	1.79×10^{12}	1.02×10^{12}	169	33	[*Hidalgo et al.,* 2000]
270	00	5.5×10^{12}	–	180	0	[*Wu et al.,* 1999]

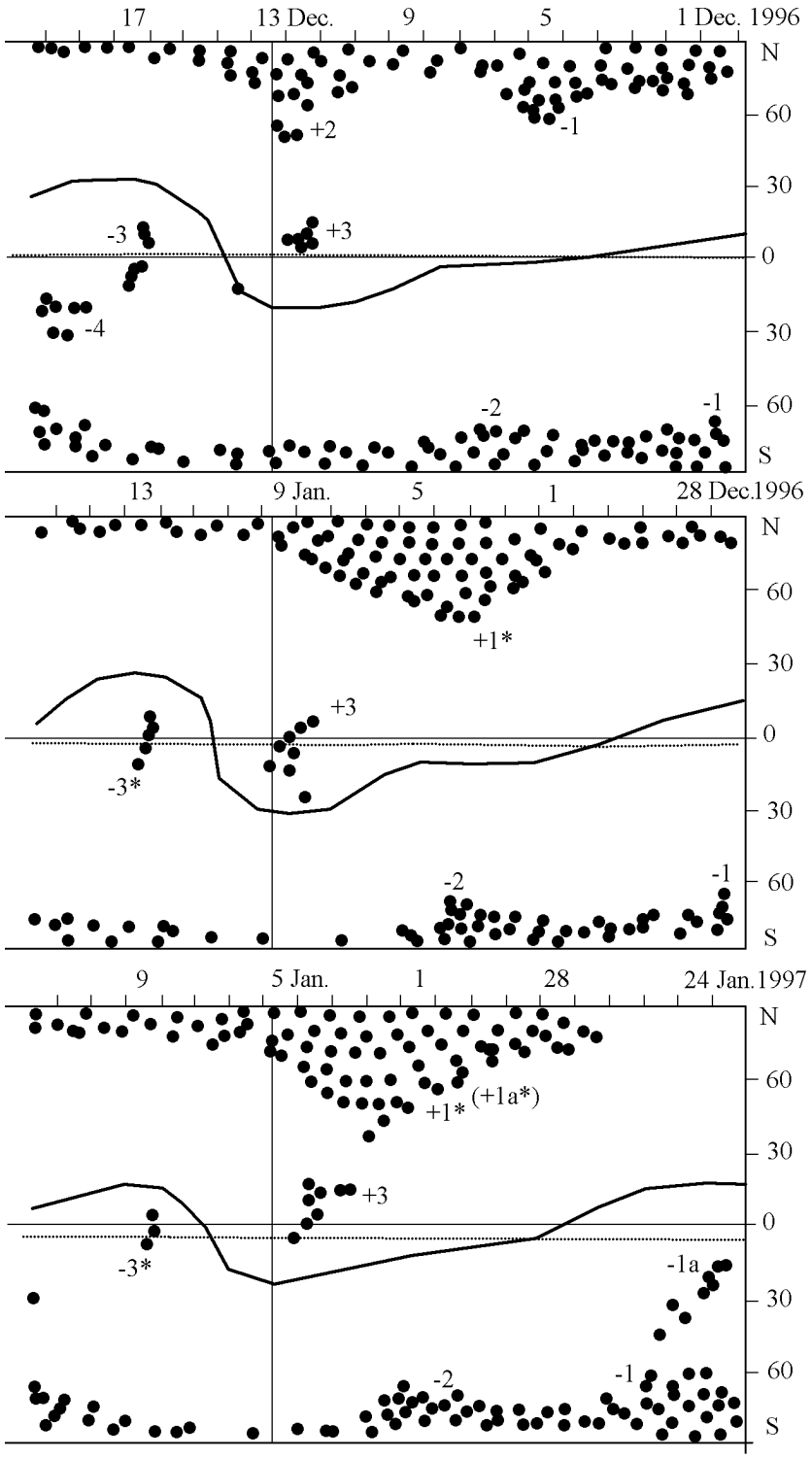

Figure 1. Photospheric regions (OR) of the open field lines of the solar magnetic field (black small circles). ± 1, $\pm 2 \ldots$ is the numeration of the regions (the plus sign means that the field is directed from the Sun). The OR dynamics in a sequence of three orbits centered on 13 December 1996, 9 January and 5 February 1997 is shown.

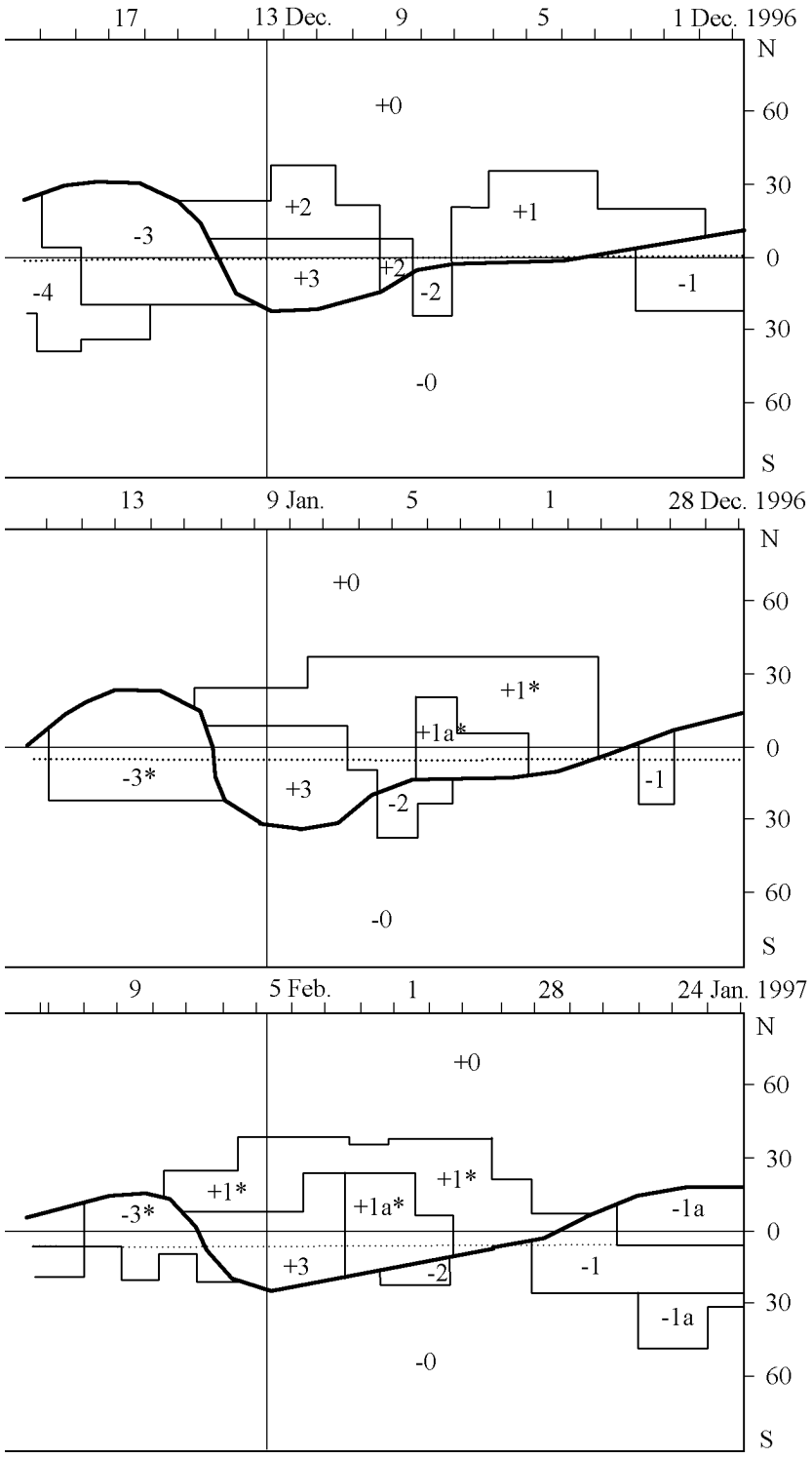

Figure 2. Subsector structure of the coronal magnetic field on the source surface ($2.5R_0$ from the center of the Sun). Intersector boundaries are shown by thin lines. The numeration corresponds to OR-sources on the photosphere. ± 0 are subsectors of the open lines from the polar cap photospheric regions.

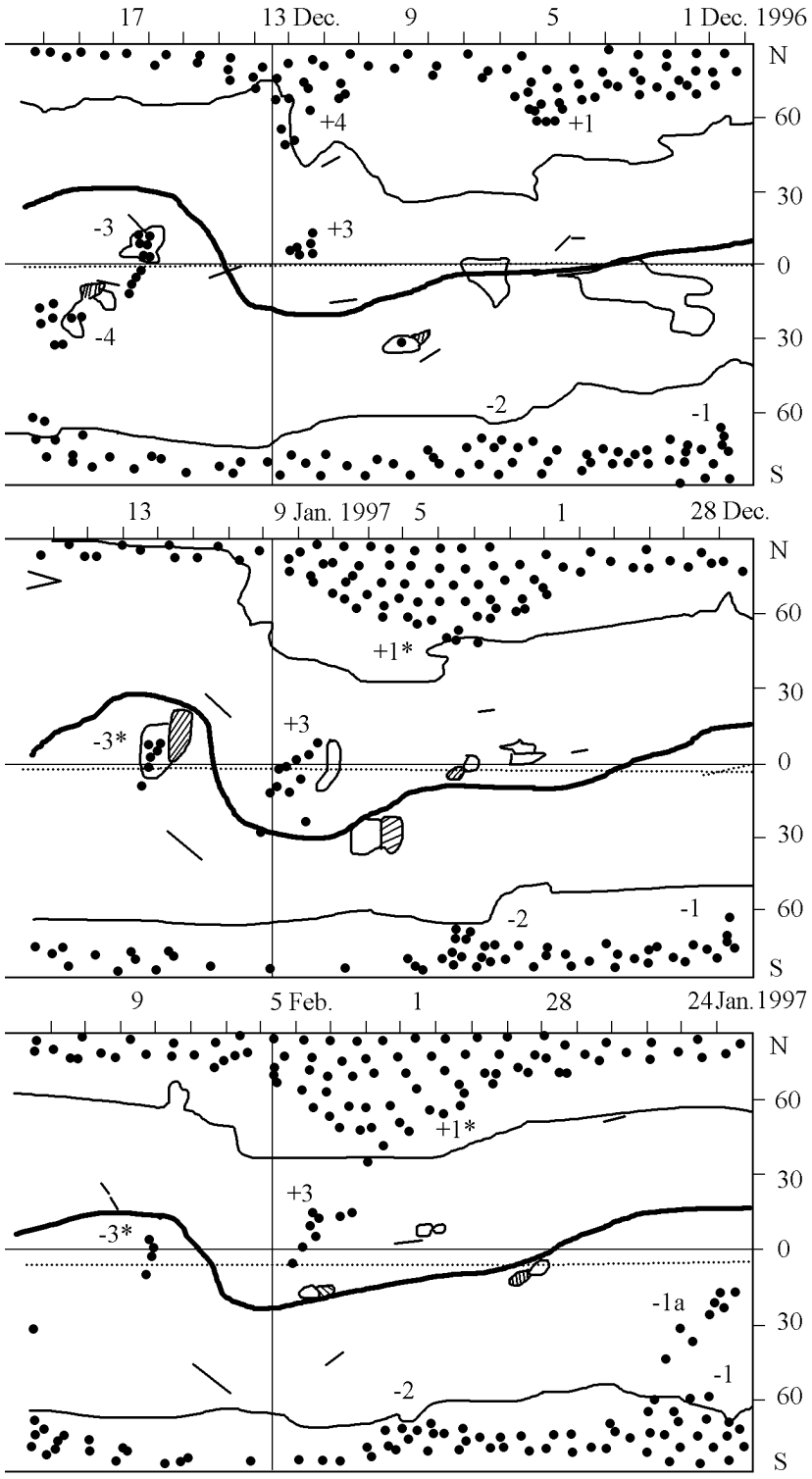

Figure 3. Mutual position of photospheric OR, coronal holes (boundaries are shown by thin curves), active regions and filaments (line segments).

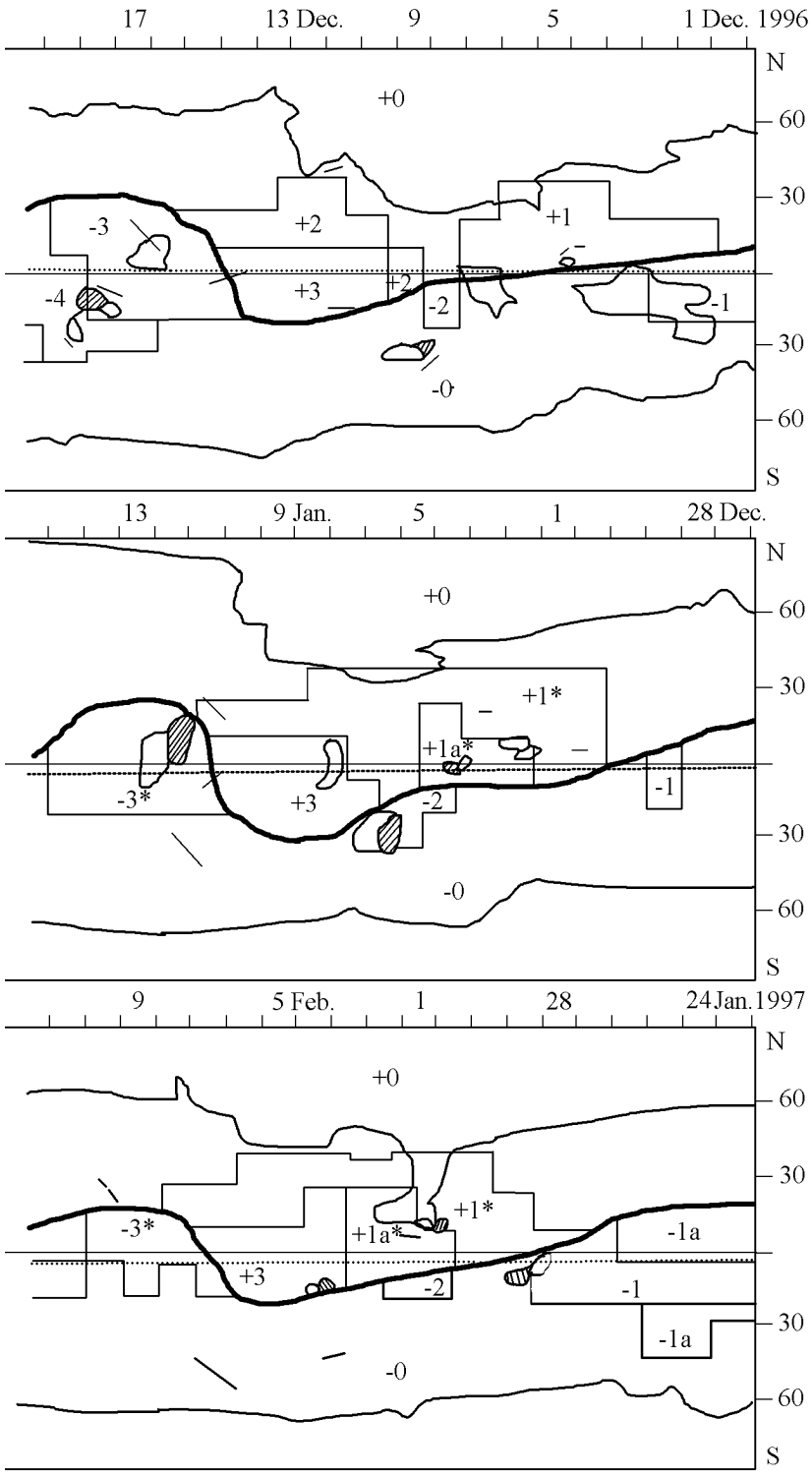

Figure 4. Position of coronal holes, active regions and filaments relative the intersector boundaries of the coronal magnetic field on the source surface.

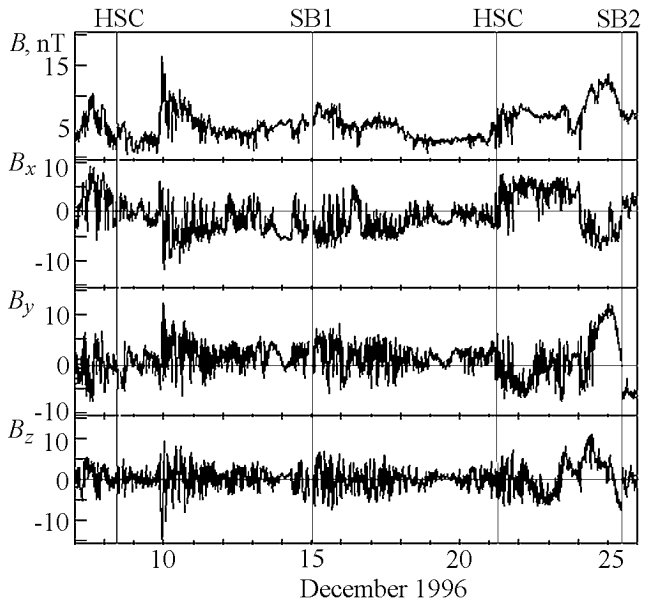

Figure 5. Variations of the IMF B, B_X, B_Y, and B_Z components (1-min averages) based on the measurements on board the Wind satellite in December 1996 (HCS and SB are the sector and intersector boundaries, respectively).

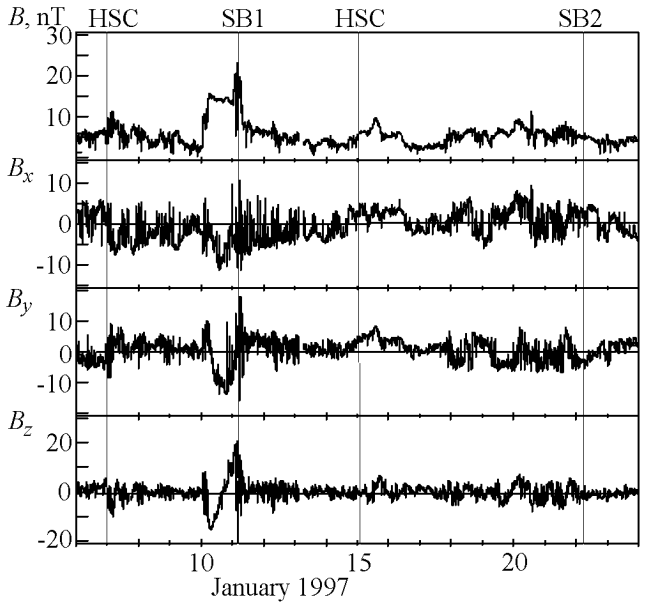

Figure 6. The same as in Figure 5 but in January 1997.

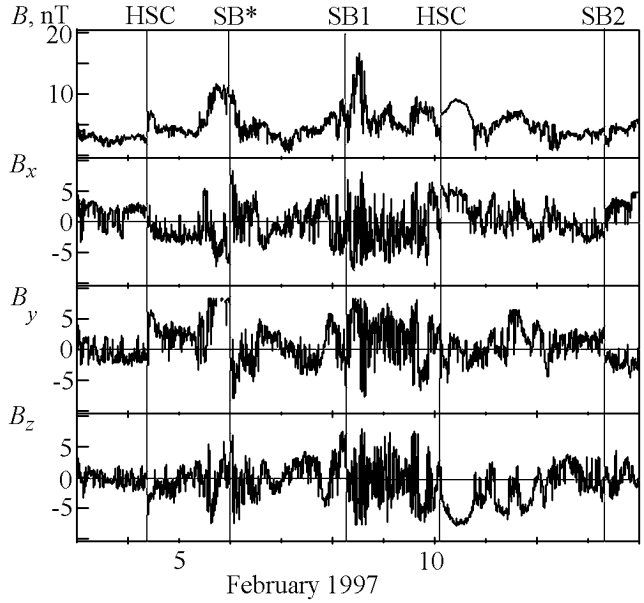

Figure 7. The same as in Figure 5 but in February 1997.

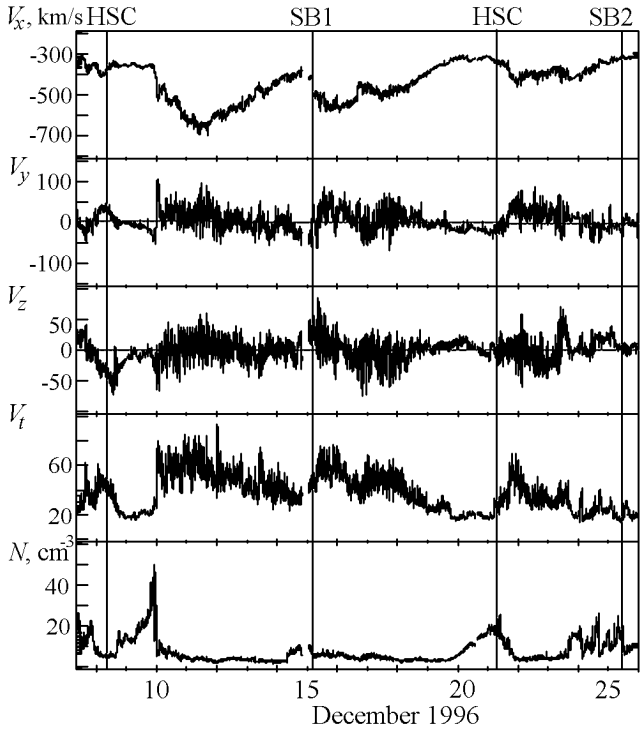

Figure 8. Variations of the V_x, V_y, and V_z components of the stream velocity (in solar-elliptic coordinates), thermal velocity V_T, and concentration N of the solar wind protons (1-min averages of the measurements on board the Wind satellite) in December 1996.

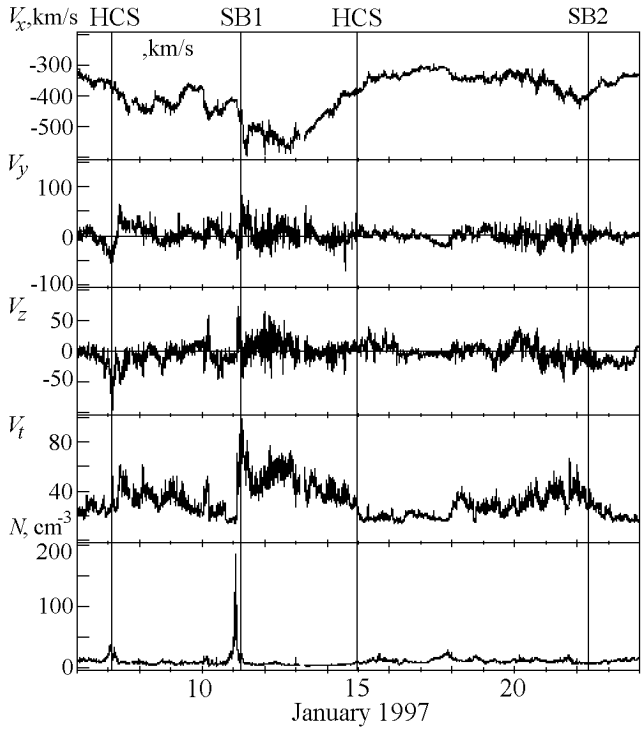

Figure 9. The same as in Figure 8 but in January 1997.

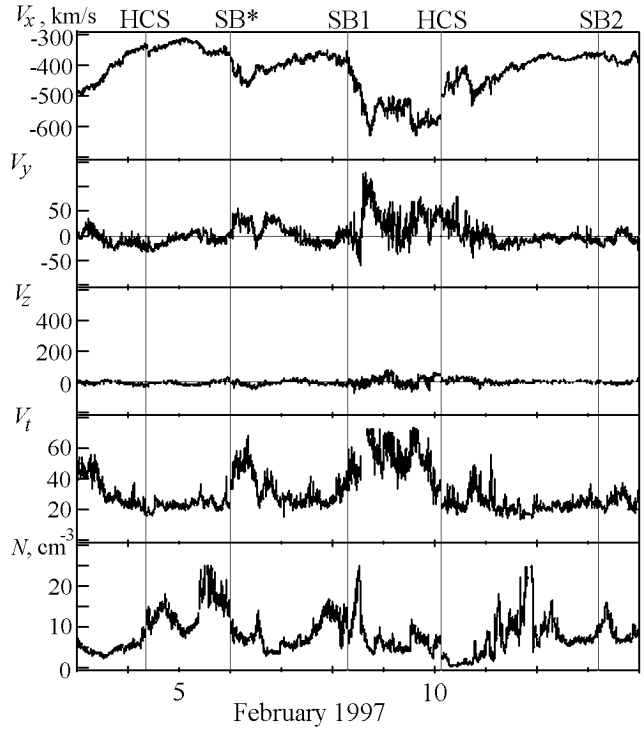

Figure 10. The same as in Figure 8 but in February 1997.

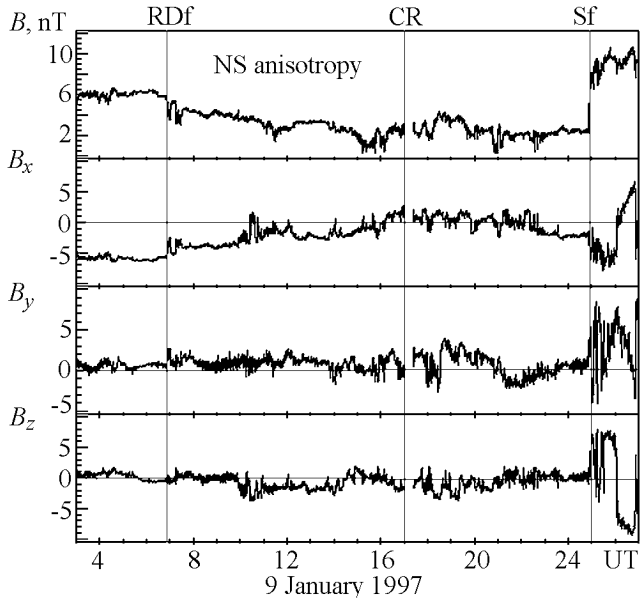

Figure 11. Variations of the IMF B, B_x, B_y, and B_z components (1-min averages of the measurements on board the Wind satellite) at the growth phase of a heliospheric substorm. R_f and S_f are the forward rotational break and shock front, respectively. RDF–CR is an interval of the north–south (NS) anisotropy of the galactic cosmic rays (GCR) [*Bieber and Evenson*, 1998].

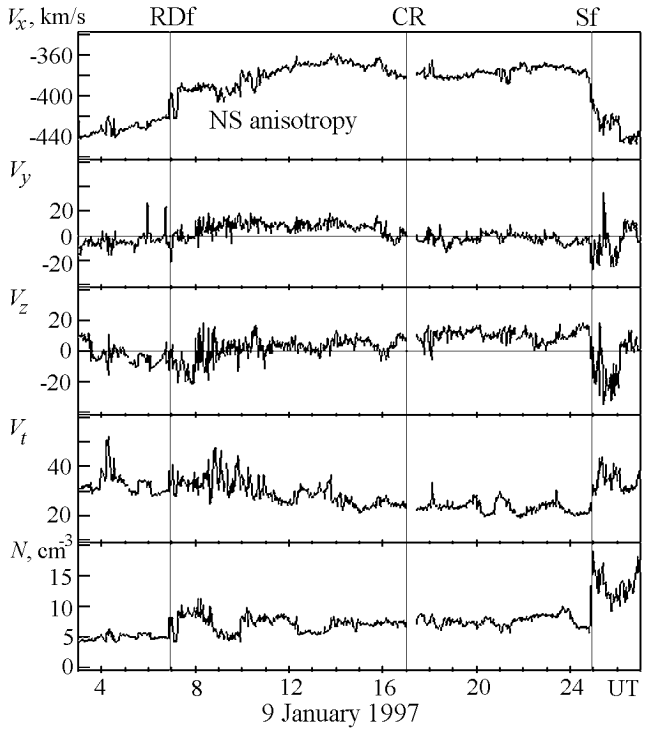

Figure 12. Variations of the V_x, V_y, and V_z components of the stream velocity, thermal velocity V_T, and concentration N of the solar wind protons at the growth phase of a heliospheric substorm. The designations are the same as in Figure 11.

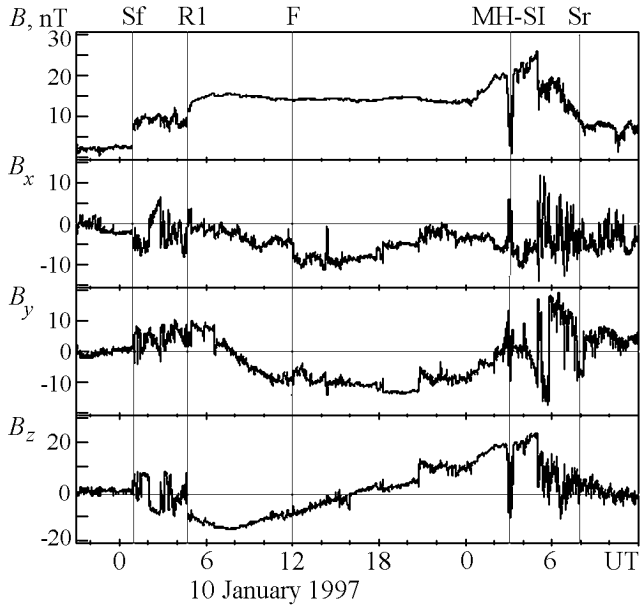

Figure 13. Variations of the IMF B, B_X, B_Y, and B_Z components according to the measurements on board the Wind satellite during the passage of the forward shock wave S_f, cloud magnetopause R_1, MHD front F, cloud rear wall (MH–SI), and reverse wave (S_r).

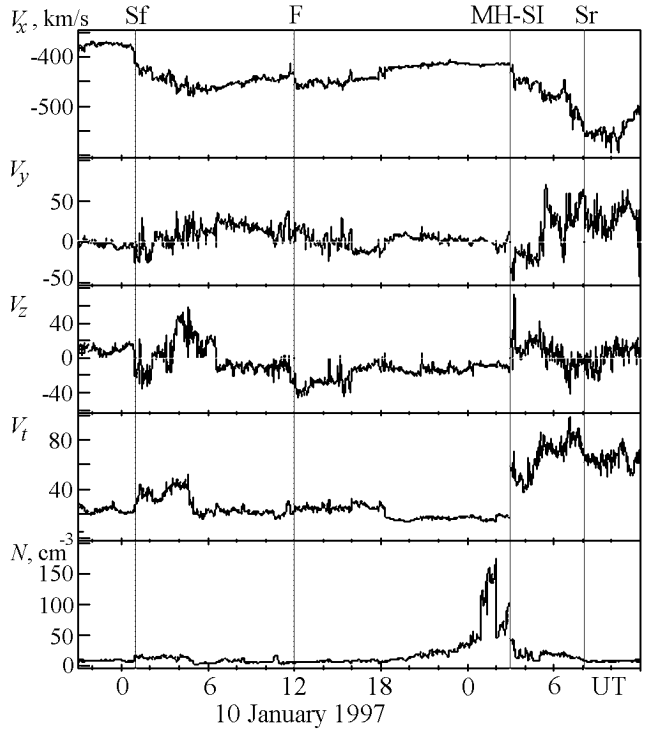

Figure 14. Variations of the V_x, V_y, and V_z components of the velocity, thermal velocity V_T, and configuration of the solar wind protons during the Wind satellite crossing the magnetic cloud and its vicinities. The designations are the same as in Figure 13.